3D numerical model for heat conduction analysis based on IR thermography

by I. Boras, S. Švaić

Faculty of Mechanical Engineering and Naval Architecture, University of Zagreb
Ivana Lučića 5, 10 000 Zagreb, Croatia

Abstract

A 3 D model based on control volume numerical method was used to simulate the heat conduction in a flat metal plate containing artificial defects. The plate was made of steel with known thermal properties and the defects of different depth were flat bottom holes simulating areas damaged by corrosion.

The result of simulation was the temperature distribution on both the intact and the damaged rear side of the plate. The temperature distribution on the metal plate surfaces depends on material properties, start and boundary conditions, heat stimulation intensity, and duration. The goal of the research was to find if there is a possibility to combine pulse-thermography (a technique which is being used since many years) and numerical modeling to determine the degree of hidden corrosion on the rear surface of a thin metal plate.

1. Introduction

For maintenance procedures and preventive measures on metal constructions the possibility to locate hidden corrosion is of considerable interest. Besides the location of such spots the estimation of material loss is very important [1].

This paper presents the results of an analysis obtained by numerical simulation for a metal plate with flat bottom holes drilled from the rear surface, which represent corrosion of different intensity. For the numerical part of the research the corrosion is defined as the reduction in material thickness neglecting any changes in thermal properties of the material that may occur due to chemical reactions involved in the corrosion process [1].

In our simulation the plate was stimulated with pulse heat flux having constant intensity over a defined time [2]. The heat flux illuminates the intact front surface while the rear surface is damaged. The temperature response on this reference surface has been monitored after heat stimulation. The defects and plate edges were arranged in such a way that their heat flow patterns did not affect each other.

2. The concept of the model

The model was a 120 x 80 x 3 mm sized flat steel plate (see figure1.) with thermal conductivity 32 W/(mK), thermal diffusivity $1,65 \cdot 10^{-5}$ m^2/s. Each of the six flat bottom holes has 10 mm diameter. The depth of each defect represents the particular loss of material caused by corrosion.

3. Start and boundary conditions

The flat plate was vertically placed in the surrounding of known temperature. The heat transfer from lateral sides of the plate was neglected (adiabatic boundary conditions). The front smooth surface was stimulated at the beginning of simulation with pulse heat flux having a total energy of 960 J over a 5 ms time interval. It is assumed that the stimulation is uniform. The rear surface was surrounded with ambient air of known temperature.

For both surfaces free convection and radiation exchange with its surrounding has been assumed. Free convection models, depending on the geometrical position of the defined control volume are used for solving the convection heat transfer.

For vertical surfaces the Mc Adams relation was used (1).

$$Nu_L = c \cdot Ra_L^m = c \cdot (Gr \cdot Pr)^m \qquad (1)$$

In this relation the Rayleigh number Ra depends on constants c and m, which are:

$c = 0.59$	$m = 1/4$	for	$10^4 \leq Ra \leq 10^9$
$c = 0.1$	$m = 1/3$	for	$10^9 \leq Ra \leq 10^{10}$

The thermal properties for air are evaluated as:

$$\vartheta_m = \frac{\vartheta_s + \vartheta_\infty}{2} \qquad (2)$$

For horizontal surfaces the Mc Adams and Goldstein relations were used. If the observed surface was oriented upside the relation (3) is used. If the observed surface is oriented downside the relation (4) is used.

$$Nu_L = 0.54 \cdot Ra_L^{1/4} \qquad 2.6 \cdot 10^4 < Ra_L < 10^7$$

$$Nu_L = 0.15 \cdot Ra_L^{1/3} \qquad 10^7 < Ra_L < 3 \cdot 10^{10} \qquad (3)$$

$$Nu_L = 0.27 \cdot Ra_L^{1/4} \qquad 3 \cdot 10^5 < Ra_L < 3 \cdot 10^{10} \qquad (4)$$

The thermal properties for air are evaluated as in (2).

The heat transfer by radiation was calculated by involving the radiation heat transfer coefficient (5).

$$\alpha_r = \frac{\varepsilon \cdot \sigma \cdot 10^{-8} \cdot (T_s - T_{ob})}{T_s - T_\infty} \qquad (5)$$

The total heat transfer coefficient was calculated as

$$\alpha_{tot} = \alpha_k + \alpha_r \qquad (6)$$

4. Statements of the numerical analysis

The problem was solved numerically by the control volume numerical method [3]. The Gauss-Seidel method was used for solving the system of algebraic equations. The total number of control volumes was 29 120. The control volume net was adopted according to the observed problem. The net was condensed in the areas where higher temperature gradients are expected [4-6].

The time step of 1 ms was adapted to the requirements given for the stability and accuracy of the discrete equation.

5. Results of the numerical analysis

Figure 3 shows the temperature evaluation on the front plate surface over the sound area for six selected positions after absorption of the heat pulse of 10^5 J/m². Due to the very short heat impulse the temperature rise is faster than its decay. The same behavior can be seen in literature [1]. The heat transfer from the illuminated front surface and the rear surface containing corrosion defects consists of natural convection and radiation. In total the heat transfer coefficient radiation is more intensive at higher temperatures and it is reduced at lower temperatures. The coefficient of convection heat transfer remains almost constant.

Figure 4 shows the temperature distribution versus time for seven locations on the plate. For selected positions (x, y) the temperatures on front and back side have been calculated. Six of them are in the center of the defects and the seventh is on the sound area. It can be seen that the temperatures at all observed points have a fast drop after heating has stopped. This temperature drop became slower and slower as the influence of defects became evident. Also on the rear surface the time correlated with the temperature maximum shifts as a function of defect depth.

Figure 5 displays the front surface temperature difference between defect and non-defect area ("temperature contrast" $\Delta T = T_d - T_{nd}$). The points where T_d was calculated were on top of each defect while the points where T_{nd} was recorded were beside each defect. The time where maximum temperature difference occurs is a function of the relative material loss $\Delta L/L$. This is very important information because the intensity of heat flux used for stimulation must be selected according to the resolution of the thermography camera.

Figure 6 displays the numerically obtained evaluation of current contrast versus time i. The data were calculated using relation (7) [1].

$$C_{3D} = \frac{T(x,y,t) - T(x_o, y_o, t)}{T(x_o, y_o, t)} \tag{7}$$

where $T(x, y, t)$ relates to the center of each defect and $T(x_0, y_0, t)$ to the sound area next to it. The time of maximal contrast rises with reducing of relative material loss (Fig.6).

Developed software allows us to observe not only the temperature change versus time in arbitrarily selected points, but also the temperature distribution on the metal plate surface in defined time intervals. Fig. 7 shows the temperature distribution recorded in various times (100 ms, 400 ms, 600 ms, and 1000 ms).

In figure 8 the three-dimensional temperature distribution of the front side of the plate is given for $t = 1000$ ms.

On figure 9 the linear temperature distribution can be seen along the $y = 60$ mm coordinate through the centers of the defects representing 50 %, 30 % and 20 % relative material loss.

6. Conclusion

The possibilities to determine hidden corrosion and to estimate its intensity using numerical method and pulse-thermography was the idea of the research presented. The paper presents results obtained with a numerical method based on 3D non-stationary heat transfer to determine simulated defects caused by corrosion. Besides relatively very small differences in material thickness the result still gives the temperature differences on the surface opposite to the corroded one. This gives the possibility for developing a procedure to determine the intensity and duration of a heat pulse according to the thermal properties of an object, boundary conditions, and IR camera characteristic. This is very important because the experimental limit for flash thermographic technique in detection corrosion has been found to be about 20 % of material loss (in steel) [1].

REFERENCES

[1]   E. Grinzato, V. Vavilov, Corrosion evaluation by thermal image processing and 3D modelling, Rev. Gen. Therm. Paris, France, pp. 669-679,1998.

[2]   D.P. Almond, P.M. Patel, *Photothermal Science and Technique*, London, Chapman & Hall, 1996.

[3]   S.V. Patankar, *Numerical Heat Transfer and Fluid Flow*, Hemisphere Publishing Corporation, Washington, 1980.

[4]   I. Boras, S. Svaic, *Determination of the Defect Parameters in Specimen by Means of Thermography and Numerical Methods*, Proceeding of The International Society for Optical Engineering, San Antonio, Texas, USA, Vol. 3396, pp. 271-281, 1998.

[5]   I. Boras, S.Svaic, A.Galovic, *Mathematical model for simulation of defects under material surface applied to thermographic measurements*, Quantitative Infrared Thermography, QIRT 98, Lodz, Poland, pp. 53-58, 1998.

[6]   I. Boras, S. Svaic, *Thermal non-destructive testing (TNDT) quantification of subsurface defects*, 11th International conference on Thermal Engineering and Thermogrammetry, Budapest, Hungary, pp. 220-225, 1999.
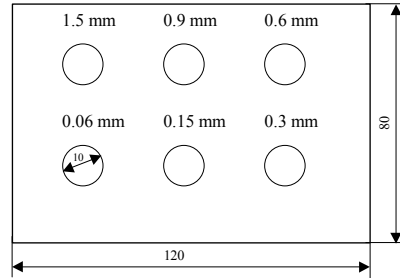
Fig. 1. *The geometrical characteristic of the plate and the defects depth. Numbers at the circles indicate depth of hole underneath the surface*
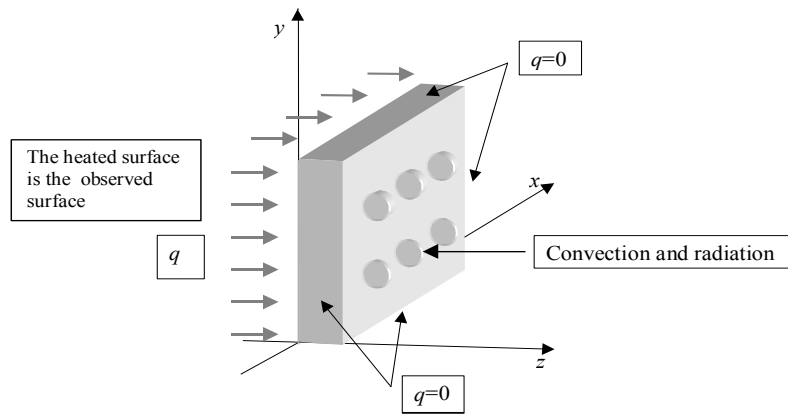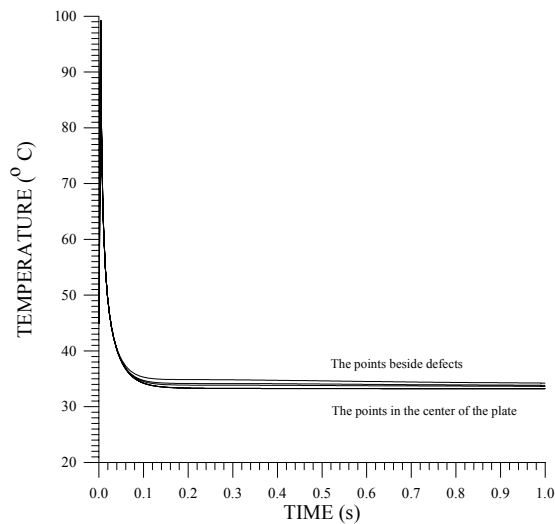

Fig. 2. *Boundary conditions*

Fig. 3. *Numerically obtained temperature change on the metal plate surface without defects, after heat pulse of 10^5 J/m^2*
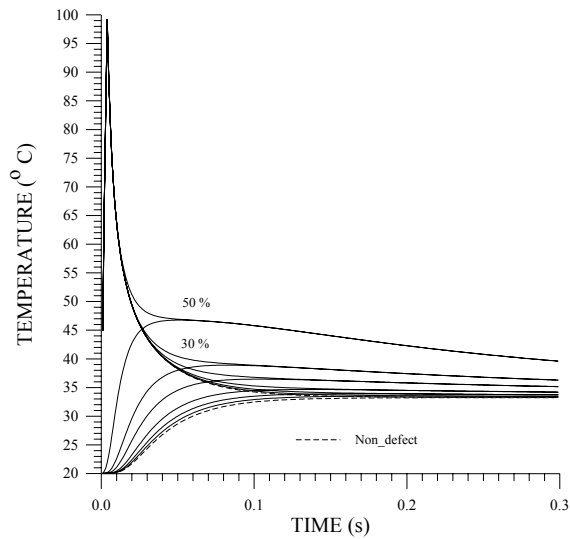
168

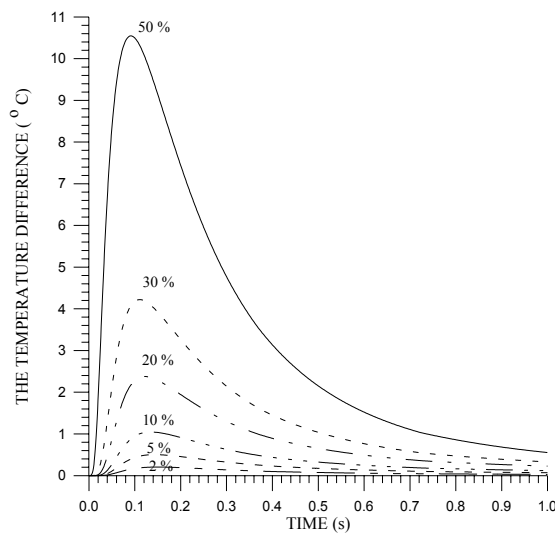**Fig. 4.** *Temperature versus time for chosen position (x, y) at front and back side of a metal*

Fig. 5. *Numerically obtained temperature difference – time relation for various material loss of 3 mm thick metal plate*
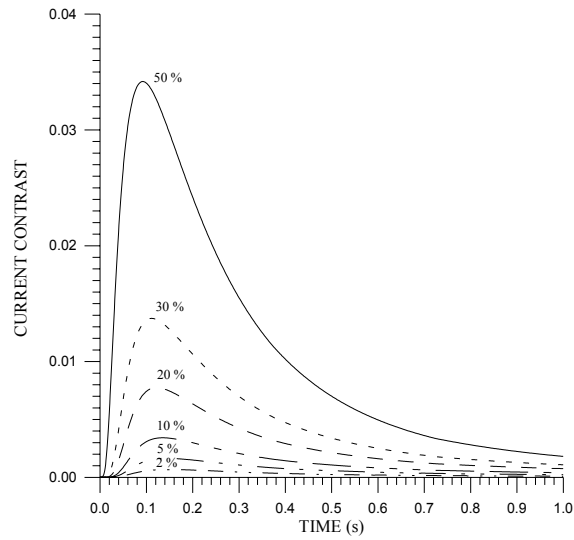
169
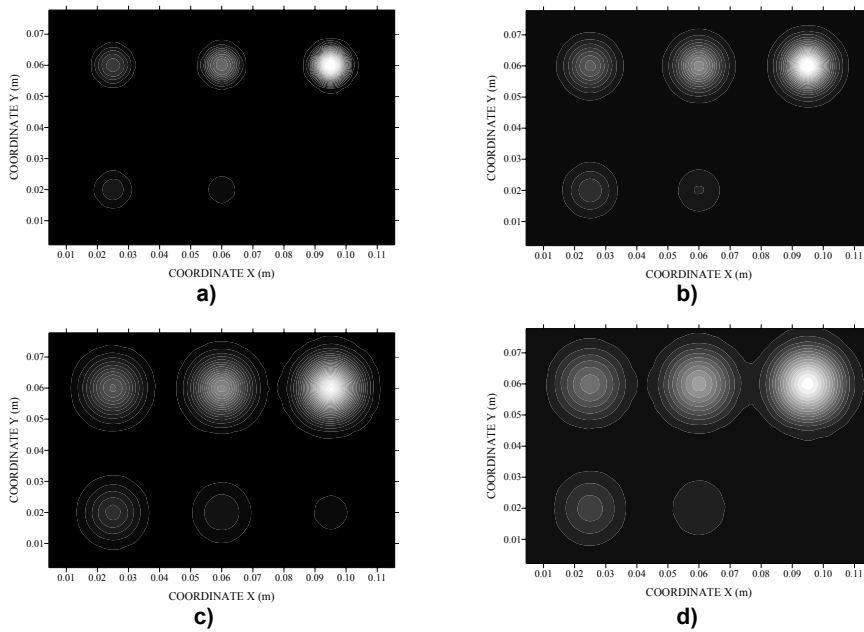
Fig. 6. Current contrast versus time

Fig. 7. Numerically obtained surface temperature distribution for sample in Fig. 1 at t a) 100 ms, b) 400 ms c) 600 ms and d) 1000 ms after illumination
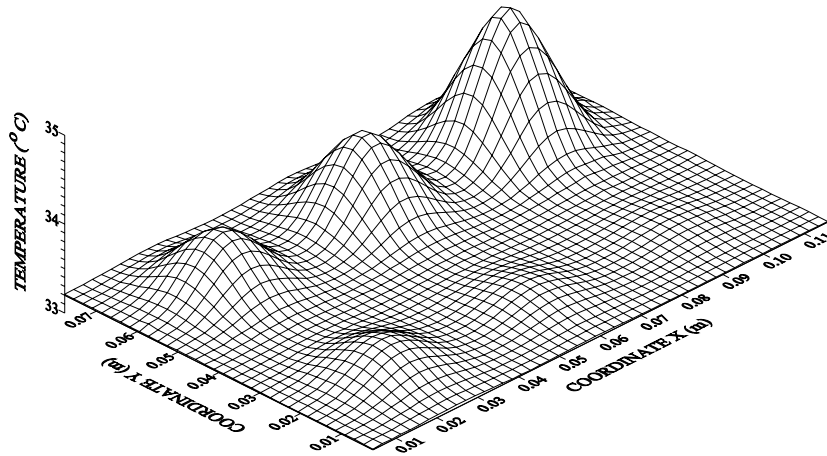
170

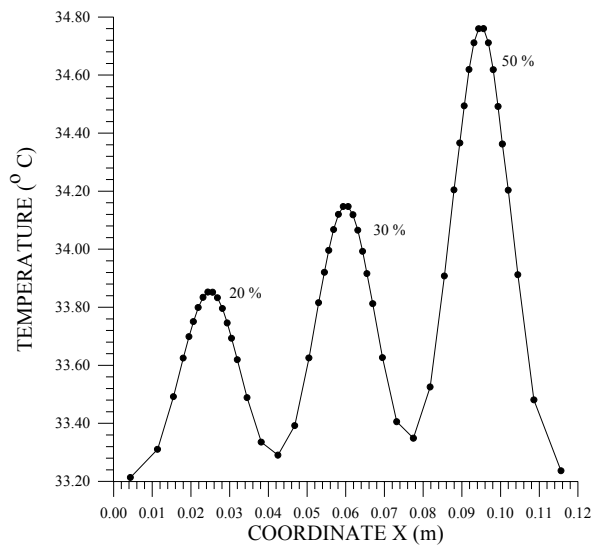**Fig. 8.** *3D temperature distribution on front surface at* t *= 1000 ms*

Fig. 9. *Linear temperature distribution along coordinate* y *= 60 mm at* t *= 1000 ms*

171